

Stability analysis of multiple-lattice self-anticipative density integration effect based on lattice hydrodynamic model in V2V environment

Geng Zhang(张埂) and Da-Dong Tian(田大东)

Citation: Chin. Phys. B, 2021, 30 (**12**): 120201. DOI: 10.1088/1674-1056/ac05b4
Journal homepage: http://cpb.iphy.ac.cn; http://iopscience.iop.org/cpb

What follows is a list of articles you may be interested in

Consistent Riccati expansion solvability, symmetries, and analytic solutions of a forced variable-coefficient extended Korteveg-de Vries equation in fluid dynamics of internal solitary waves

Ping Liu(刘萍), Bing Huang(黄兵), Bo Ren(任博), and Jian-Rong Yang(杨建荣)
Chin. Phys. B, 2021, 30 (**8**): 080203. DOI: 10.1088/1674-1056/ac052a

Closed form soliton solutions of three nonlinear fractional models through proposed improved Kudryashov method

Zillur Rahman, M Zulfikar Ali, and Harun-Or Roshid
Chin. Phys. B, 2021, 30 (**5**): 050202. DOI: 10.1088/1674-1056/abd165

Bright and dark soliton solutions for some nonlinear fractional differential equations

Ozkan Guner, Ahmet Bekir
Chin. Phys. B, 2016, 25 (**3**): 030203. DOI: 10.1088/1674-1056/25/3/030203

Complex dynamical behaviors of compact solitary waves in the perturbed mKdV equation

Yin Jiu-Li, Xing Qian-Qian, Tian Li-Xin
Chin. Phys. B, 2014, 23 (**8**): 080201. DOI: 10.1088/1674-1056/23/8/080201

Nonlocal symmetry, optimal systems, and explicit solutions of the mKdV equation

Xin Xiang-Peng, Miao Qian, Chen Yong
Chin. Phys. B, 2014, 23 (**1**): 010203. DOI: 10.1088/1674-1056/23/1/010203

Stability analysis of multiple-lattice self-anticipative density integration effect based on lattice hydrodynamic model in V2V environment*

Geng Zhang(张埂)[1] and Da-Dong Tian(田大东)[2,†]

[1] College of Computer and Information Science, Southwest University, Chongqing 400715, China
[2] College of Information Science and Engineering, Shandong Agricultural University, Tai'an 271018, China

(Received 11 March 2021; revised manuscript received 23 April 2021; accepted manuscript online 27 May 2021)

Under the environment of vehicle-to-vehicle (V2V) communication, the traffic information on a large scale can be obtained and used to coordinate the operation of road traffic system. In this paper, a new traffic lattice hydrodynamic model is proposed which considers the influence of multiple-lattice self-anticipative density integration on traffic flow in the V2V environment. Through theoretical analysis, the linear stability condition of the new model is derived and the stable condition can be enhanced when more-preceding-lattice self-anticipative density integration effect is taken into account. The property of the unstable traffic density wave in the unstable region is also studied according to the nonlinear analysis. It is shown that the unstable traffic density wave can be described by solving the modified Korteweg–de-Vries (mKdV) equation. Finally, the simulation results demonstrate the validity of the theoretical results. Both theoretical analysis and numerical simulations demonstrate that multiple-lattice self-anticipative density integration effect can enhance the stability of traffic flow system in the V2V environment.

Keywords: lattice hydrodynamic model, traffic stability, self-anticipative density integration, mKdV equation

PACS: 02.30.jr, 45.70.Vn **DOI:** 10.1088/1674-1056/ac05b4

1. Introduction

Lots of traffic problems are caused by the contradiction between the finite road resource and the increasing demand for traffic construction in our daily life. In order to reduce traffic problem, we need to find out the origin of traffic problem and the operation rule of the traffic system. A natural way of describing the road traffic is the micro traffic modeling, which mainly describes a single vehicle's motion process and its influence factors. Another way is the macro traffic modeling, which primarily depicts the road traffic as compressible fluid, and then the traffic characteristics are studied according to traffic wave theory.

In 1995, on the assumption that the following vehicle's motion depends mainly on the headway between the considered vehicle and its preceding vehicle, Bando *et al.*[1] constructed an optimal velocity function and proposed a famous optimal velocity car-following model. Then, Nagatani[2] introduced the idea of the optimal velocity car-following model into the macro traffic modeling and proposed the lattice hydrodynamic model. Since then, lots of modified traffic models have been constructed to reveal the influence of different traffic factors on traffic flow.[3–15] For example, Dong *et al.*[3] constructed a hybrid traffic flow model at an off-ramp bottleneck by considering the adaptive cruise control vehicles and cooperative adaptive cruise control vehicles. Peng[4] investigated the effect of traffic interruption probability on traffic flow based on a new optimal velocity car-following model by considering the driver's anticipation effect of traffic interruption probability. Chen and Zhang[5] proposed a traffic flow dynamics model and studied the physical phenomenon of high-speed car following behavior. Jin *et al.*[6] explored the nonlinear density wave and energy consumption for a curved road by taking the friction coefficient and the road curvature into account. Gupta *et al.*[7] analyzed the traffic evolution properties of a lattice traffic flow model on a gradient highway. Ge and Cheng[11] introduced an improved lattice hydrodynamic model considering the effect of "backward looking". Tian *et al.*[12] extended the original lattice hydrodynamic model by considering the density difference effect. Wang *et al.*[15] studied the traffic flow evolution rule for two-lane traffic system by introducing a modified two-lane lattice hydrodynamic model.

Recently, in order to improve the stability of traffic flow, the lattice hydrodynamic modeling on the basis of control theory was studied. In 2015, Ge *et al.*[16] applied the delayed-feedback control method to the lattice hydrodynamic model proposed by Nagatani.[2] Li *et al.*[17] and Qin *et al.*[18] respectively studied the effects of density change rate and flux change rate on traffic flow by the Laplace transform method. Liu *et al.*[19] studied the lattice hydrodynamic model-based traffic control from the perspective of transportation cyber-physical system approach. Pan *et al.*[20] introduced a delay-independent traffic flux control method into a discrete-time lat-

*Project sponsored by the Natural Science Foundation of Chongqing, China (Grant No. cstc2019jcyj-msxmX0265).
†Corresponding author. E-mail: dadong@sdau.edu.cn
© 2021 Chinese Physical Society and IOP Publishing Ltd

tice hydrodynamic model with time-delay. It is revealed that the controlled traffic system can run much more steadily.

In fact, the driving process is continuous in real traffic. The influence of some continuous traffic information on traffic flow has also been studied. In 2018, Zhao *et al.*[21] presented a new lattice hydrodynamic model by introducing the continuous historical current integration information into macro traffic modeling. Later, He *et al.*[22] uncovered the effect of density integration on the stability of a new lattice hydrodynamic model. In addition, the influences of continuous traffic flux and density information on traffic flow have been studied by Wang *et al.*[23] and Qi *et al.*[24] Besides the relative continuous traffic information of two successive lattices, Liu *et al.*[25] investigated the stabilization effect of self-delayed flux integral for the two-lane lattice hydrodynamic model. But the continuous traffic information considered in the above models are delayed traffic information. In 2017, Zhang *et al.*[26] presented a new lattice hydrodynamic model in which the lattice self-anticipative density effect is considered, and they also attested to the stabilization effect of lattice self-anticipative density on traffic flow.

However, the lattice self-anticipative density effect in Ref. [26] was proposed for a single lattice at a fixed time. In fact, the development of intelligent transportation system and the vehicle-to-vehicle (V2V) communication technology show that the considered vehicle movement is adjusted not only by the nearby traffic information, but also by the information obtained from far preceding vehicles. So, it is more reasonable to study the traffic evolution property with consideration of multiple anticipative traffic information acquired in a continuous time interval in the V2V environment. But little work on the effect of multiple-lattice self-anticipative information on the traffic flow from the viewpoint of V2V communication environment was done. Therefore, in this paper, a new lattice hydrodynamic model is proposed by considering the multiple-preceding-lattice continuous self-anticipative density information, and the new model's stability condition and the density wave propagation rules are discussed as well.

The rest of this paper is organized as follows. In Section 2, the new model is presented. In Section 3 the new model's linear and nonlinear properties are analyzed. The numerical simulation is presented in Section 4, and some conclusions are drawn in Section 5.

2. New model

The lattice hydrodynamic model proposed by Nagatani[2] in 1998 is given by the following equations:

$$\partial_t \rho_j + \rho_0 \left(\rho_j v_j - \rho_{j-1} v_{j-1}\right) = 0, \tag{1}$$

$$\partial_t (\rho_j v_j) = a\rho_0 V(\rho_{j+1}) - a\rho_j v_j, \tag{2}$$

where ρ_j and v_j are the density and velocity of lattice j at time t respectively, ρ_0 is the average density, a denotes driver's sensitivity, and V represents the optimal velocity function. A widely used expression of the optimal velocity function is given by

$$V(\rho_j) = \frac{v_{\max}}{2}\left[\tanh\left(\frac{2}{\rho_0} - \frac{\rho_j}{\rho_0^2} - \frac{1}{\rho_c}\right) + \tanh\left(\frac{1}{\rho_c}\right)\right], \tag{3}$$

where $v_{\max}$ is the maximal velocity and ρ_c is the critical density.

The lattice hydrodynamic model has been widely extended since it was proposed. Among the extended researches, an important model is constructed by taking the relative density difference information into account and the governing equation of this model is[12]

$$\partial_t \rho_j + \rho_0 \left(\rho_j v_j - \rho_{j-1} v_{j-1}\right) = 0, \tag{4}$$

$$\partial_t (\rho_j v_j) = a\rho_0 V(\rho_{j+1}) - a\rho_j v_j + \lambda \left(\rho_j - \rho_{j+1}\right)/\rho_0, \tag{5}$$

where λ is a coefficient and $\rho_j - \rho_{j+1}$ is the relative density difference between lattices j and $j+1$.

In the above model, the density difference information is mainly from two successive lattices. Recently, Zhang *et al.*[26] considered the influence of driver's self-anticipative density information on traffic stability and presented the following model:

$$\partial_t \rho_j + \rho_0 \left(\rho_j v_j - \rho_{j-1} v_{j-1}\right) = 0, \tag{6}$$

$$\partial_t (\rho_j v_j) = a\rho_0 V(\rho_{j+1}) - a\rho_j v_j + ak\left(\rho_{j+1} - \rho_{j+1}(t+\tau_0)\right)/\rho_0, \tag{7}$$

where τ_0 is the anticipative time, $\rho_{j+1} - \rho_{j+1}(t+\tau_0)$ denotes the self-anticipative density difference of lattice $j+1$, and k is the reaction coefficient.

The self-anticipative density information in Zhang's model is set to be at a fixed time. But in real traffic situation, the road traffic motion process is a continuous process. So, it is more reasonable to study the continuous anticipative traffic information on traffic flow. On the other hand, in the V2V environment, multiple-preceding-vehicles traffic information can be obtained and used for the considered vehicle to adjust its motion behavior. In view of these reasons, a new lattice hydrodynamic model by considering the effect of multiple-lattice self-anticipative density integration is presented as

$$\partial_t \rho_j + \rho_0 \left(\rho_j v_j - \rho_{j-1} v_{j-1}\right) = 0, \tag{8}$$

$$\partial_t (\rho_j v_j) = a\rho_0 V(\rho_{j+1}) - a\rho_j v_j + \frac{\gamma}{\rho_0}\sum_{p=1}^{m}\int_{s=0}^{t_0} \left(\rho_{j+p}(t) - \rho_{j+p}(t+s)\right) \mathrm{d}s, \tag{9}$$

where m is the number of preceding lattices and γ is the reaction coefficient. The integration of the self-anticipative density means that the density information is continuous.

By linearizing the self-anticipative density term $\rho_{j+p}(t+s)$ for t, it follows that

$$\rho_{j+p}(t+s) = \rho_{j+p}(t) + s\partial_t \rho_{j+p}(t). \tag{10}$$

Then, equation (9) can be simplified in terms of Eq. (10) into the following formula:

$$\partial_t(\rho_j v_j) = a\rho_0 V(\rho_{j+1}) - a\rho_j v_j - \frac{\gamma t_0^2}{2\rho_0}\sum_{p=1}^{m}(\partial_t \rho_{j+p}(t)). \tag{11}$$

Further, by substituting Eq. (11) into Eq. (8), one has

$$\partial_t^2 \rho_j + \rho_0\left\{\left[a\rho_0 V(\rho_{j+1}) - a\rho_j v_j - \frac{\gamma t_0^2}{2\rho_0}\sum_{p=1}^{m}(\partial_t \rho_{j+p}(t))\right] - \left[a\rho_0 V(\rho_j) - a\rho_{j-1}v_{j-1} - \frac{\gamma t_0^2}{2\rho_0}\sum_{p=1}^{m}\left(\partial_t \rho_{j+p-1}(t)\right)\right]\right\} = 0. \tag{12}$$

Then, equation (12) can be rewritten into the following density dynamical equation:

$$\partial_t^2 \rho_j + a\rho_0^2\left(V(\rho_{j+1}) - V(\rho_j)\right) + a\partial_t \rho_j - \frac{1}{2}\gamma t_0^2 \sum_{p=1}^{m}\left(-\partial_t \rho_{j+p}(t) - \partial_t \rho_{j+p-1}(t)\right) = 0. \tag{13}$$

3. Theoretical analysis

3.1. Linear stability analysis

Linear stability analysis of the new model is implemented in this subsection. The analysis is carried out for a ring road. It is supposed that the traffic flow is stable when the road traffic density of every lattice is the average density ρ_0 and every vehicle on the ring road moves at the same optimal velocity $V(\rho_0)$, so the stable solution of traffic flow is

$$\rho_j(t) = \rho_0, \quad v_j(t) = V(\rho_0). \tag{14}$$

To derive the linear stability, the density of lattice j perturbed by $y_j(t)$ is expressed as

$$\rho_j(t) = \rho_0 + y_j(t). \tag{15}$$

By substituting Eq. (15) into Eq. (13), and making the resulting Eq. (13) linearized, it follows that

$$\partial_t^2 y_j + a\rho_0^2 V'\left(y_{j+1} - y_j\right) + a\partial_t y_j - \frac{1}{2}\gamma t_0^2 \sum_{p=1}^{m}\left(\partial_t y_{j+p}(t) - \partial_t y_{j+p-1}(t)\right) = 0, \tag{16}$$

where $V' = \mathrm{d}V(\rho)/\mathrm{d}\rho|_{\rho=\rho_0}$.

Let $y_j(t) = \exp(\mathrm{i}kj + zt)$ and substitute it into Eq. (16), then the differential equation of Eq. (16) will be able to be transformed into the following algebraic equation of z

$$z^2 + a\rho_0^2 V'\left(\mathrm{e}^{\mathrm{i}k} - 1\right) + az - \frac{1}{2}\gamma t_0^2 \sum_{p=1}^{m}(\mathrm{e}^{\mathrm{i}kp} - \mathrm{e}^{\mathrm{i}k(p-1)})z = 0. \tag{17}$$

Furthermore, we insert $z = z_1(\mathrm{i}k) + z_2(\mathrm{i}k)^2 + \cdots$ into Eq. (17) and derive the first-order and second-order terms of $\mathrm{i}k$ as follows:

$$z_1 = -\rho_0^2 V', \tag{18}$$

$$z_2 = -\frac{1}{a}z_1^2 - \frac{1}{2}\rho_0^2 V' + \frac{1}{2a}\gamma t_0^2 m z_1. \tag{19}$$

The linear stability depends on the value of z_2 in view of long-wavelength mode. The traffic flow is stable when $z_2 > 0$, but becomes unstable when $z_2 < 0$. So, the stable condition is

$$a > -2\rho_0^2 V' - \gamma t_0^2 m. \tag{20}$$

The neutral stability condition is

$$a = -2\rho_0^2 V' - \gamma t_0^2 m. \tag{21}$$

From Eq. (21), we can draw the neutral stability lines in the density–sensitivity space for different values of m and the result is shown in Fig. 1.

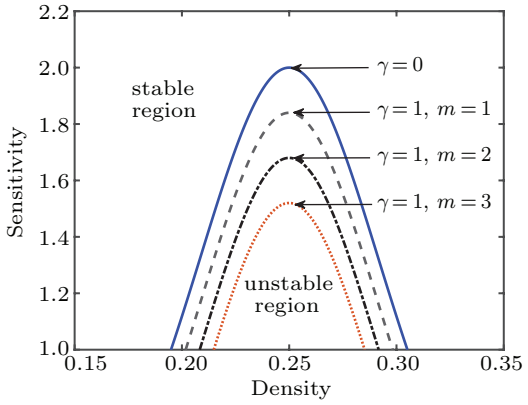


Fig. 1. Neutral stability lines in the density–sensitive space.

In Fig. 1, the neutral stability lines are derived for $m = 1$, 2, and 3 when $t_0 = 0.4$, $\gamma = 1$, $v_{\max} = 2$, $\rho_0 = \rho_c = 0.25$. Also, we consider the case when $\gamma = 0$, which is corresponding to the situation where no lattice self-anticipative density integration effect is considered. It is clear from Eq. (21) that the region above each neutral stability line is the stable region, and the region below each neutral stability line is the unstable region in Fig. 1. Also, it is observed that the neutral stability line for $\gamma = 0$ is higher than that for $\gamma \neq 0$. Moreover, the neutral stability lines go down gradually when $\gamma \neq 0$ and m increases from 1 to 3. This reveals that the unstable traffic region can be reduced by considering lattice self-anticipative density integration effect, and the unstable traffic region can be

further shrunk if more-preceding-lattice self-anticipative density integration effect is considered. In other words, the lattice self-anticipative density integration effect can improve the stability of traffic flow, and the stabilization effect is more obvious when more-preceding-lattice information is taken into account.

3.2. Nonlinear analysis

In view of the linear stability analysis result, it is clearly shown that the density–sensitive space is divided into the stable region and the unstable region. Theoretically, the traffic flow in the stable region is resistive to a small outside disturbance, but it in the unstable region will evolve into traffic congestion under a small outside disturbance. To show the form and propagation rule of the density wave in the unstable region, a long-wavelength expansion is used for the new model in the unstable region near the critical point (ρ_c, a_c). For the space variable j and time variable t, ε $(0<\varepsilon\ll 1)$ is the slow scale, the slow variables X and T are defined as

$$X=\varepsilon(j+bt),\quad T=\varepsilon^3 t, \tag{22}$$

where b is undetermined.

Let

$$\rho_j(t)=\rho_c+\varepsilon R(X,T), \tag{23}$$

substitute Eq. (23) into Eq. (13), and further expand Eq. (13) to the fifth-order of ε, then it will follow

$$\begin{aligned}
&\varepsilon^2\left(b+\rho_c^2V'(\rho_c)\right)\partial_X R\\
&+\varepsilon^3\left(\frac{1}{a}b^2+\frac{1}{2}\rho_c^2V'(\rho_c)-\frac{1}{2a}\gamma t_0^2 bm\right)\partial_X^2 R\\
&+\varepsilon^4\left[\left(\frac{1}{6}\rho_c^2V'(\rho_c)-\frac{1}{4a}\gamma t_0^2 b\sum_{p=1}^{m}\left(p^2-(p-1)^2\right)\right)\partial_X^3 R\right.\\
&\left.+\frac{1}{6}\rho_c^2V'''(\rho_c)\partial_X R^3+\partial_T R\right]\\
&+\varepsilon^5\left[\left(\frac{1}{24}\rho_c^2V'(\rho_c)-\frac{1}{12a}\gamma t_0^2 b\sum_{p=1}^{m}\left(p^3-(p-1)^3\right)\right)\partial_X^4 R\right.\\
&\left.+\left(\frac{1}{a}2b-\frac{1}{2a}\gamma t_0^2 m\right)\partial_T\partial_X R+\frac{1}{12}\rho_c^2V'''(\rho_c)\partial_X^2 R^3\right]=0,
\end{aligned}\tag{24}$$

where

$$V'(\rho_c)=\mathrm{d}V(\rho)/\mathrm{d}\rho|_{\rho=\rho_c},\quad V'''(\rho_c)=\mathrm{d}^3V(\rho)/\mathrm{d}\rho^3|_{\rho=\rho_c}.$$

In the neighborhood of the critical point (ρ_c, a_c), let $\tau=(1+\varepsilon^2)\tau_c$, $b=-\rho_c^2V'(\rho_c)$, then equation (24) will be able to be simplified into

$$\begin{aligned}
&\partial_T R-g_1\partial_X^3 R+g_2\partial_X R^3\\
&+\varepsilon(g_3\partial_X^2 R+g_4\partial_X^4 R+g_5\partial_X^2 R^3)=0,
\end{aligned}\tag{25}$$

where

$$\begin{aligned}
g_1 &= -\frac{1}{6}\rho_c^2V'(\rho_c)+\frac{1}{4a_c}\gamma t_0^2 b\sum_{p=1}^{m}\left(p^2-(p-1)^2\right),\\
g_2 &= \frac{1}{6}\rho_c^2V'''(\rho_c),\\
g_3 &= -\frac{1}{2}\rho_c^2V'(\rho_c),\\
g_4 &= \left(\frac{1}{24}\rho_c^2V'(\rho_c)-\frac{1}{12a_c}\gamma t_0^2 b\sum_{p=1}^{m}\left(p^3-(p-1)^3\right)\right)\\
&\quad-\left(\frac{1}{a_c}2b-\frac{1}{2a_c}\gamma t_0^2 m\right)\\
&\quad\times\left(\frac{1}{6}\rho_c^2V'(\rho_c)-\frac{1}{4a_c}\gamma t_0^2 b\sum_{p=1}^{m}\left(p^2-(p-1)^2\right)\right),\\
g_5 &= \frac{1}{12}\rho_c^2V'''(\rho_c)-\frac{1}{6a_c}\left(2b-\frac{1}{2}\gamma t_0^2 m\right)\rho_c^2V'''(\rho_c).
\end{aligned}$$

Adopting the following transformation:

$$T'=g_1T,\quad R=\sqrt{\frac{g_1}{g_2}}R', \tag{26}$$

equation (25) can be transformed into

$$\partial_{T'}R'-\partial_X^3R'+\partial_X R'^3+\varepsilon M\left[R'\right]=0, \tag{27}$$

where

$$M[R']=\frac{1}{g_1}\left(g_3\partial_X^2R'+g_4\partial_X^4R'+\frac{g_1g_5}{g_2}\partial_X^2R'^3\right).$$

Equation (27) is the standard modified Korteweg–de-Vries (mKdV) equation with an $O(\varepsilon)$ correction term. If we ignore the $O(\varepsilon)$ term, equation (27) is reduced to the mKdV equation with a kink–antikink solution as

$$R_0'(X,T')=\sqrt{c}\tanh\left(\sqrt{\frac{c}{2}}\left(X-cT'\right)\right), \tag{28}$$

where c is the propagation velocity for the kink–antikink solution.

By solving $(R_0', M[R_0'])\equiv\int_{-\infty}^{+\infty}\mathrm{d}XR_0'M[R_0']=0$, where $M[R_0']=M[R']$, the value of c is

$$c=\frac{5g_2g_3}{2g_2g_4-3g_1g_5}. \tag{29}$$

So, the kink–antikink solution is

$$\begin{aligned}
\rho_j &= \rho_c+\sqrt{\frac{g_1c}{g_2}\left(\frac{a_c}{a}-1\right)}\tanh\sqrt{\frac{c}{2}\left(\frac{a_c}{a}-1\right)}\\
&\quad\times\left[j+\left(1-cg_1\left(\frac{a_c}{a}-1\right)\right)t\right].
\end{aligned}\tag{30}$$

4. Numerical simulation

Numerical simulation of the new model is carried out to reveal the influence of multiple-lattice self-anticipative density integration effect on the evolution process of traffic flow. The simulation is conducted under periodic boundary condition. For convenience of simulation, we rewrite Eq. (13) into the following difference equation:

$$\rho_j(t+2\tau)=2\rho_j(t+\tau)-\rho_j(t)-\tau^2a\rho_0^2\left(V(\rho_{j+1})-V(\rho_j)\right)$$

$$
\begin{aligned}
&-a\tau\left(\rho_j(t+\tau)-\rho_j(t)\right)\\
&+\frac{1}{2}\tau\gamma t_0^2\sum_{p=1}^{m}\left(\rho_{j+p}(t+\tau)-\rho_{j+p}(t)\right.\\
&\left.-\rho_{j+p-1}(t+\tau)+\rho_{j+p-1}(t)\right),
\end{aligned}
\tag{31}
$$

where $\tau = 0.1$ is the time step.

The initial traffic condition is

$$
\rho_j(1)=\rho_j(0)=\begin{cases}\rho_0, & j\neq 100,99,\\ \rho_0-0.1, & j=100,\\ \rho_0+0.1, & j=99.\end{cases}
\tag{32}
$$

The other simulation parameters are selected as $N = 100$, $a = 1.7$, $v_{\max} = 2$, $\rho_0 = \rho_c = 0.25$, and $\tau_0 = 0.4$. The simulation results are shown in Figs. 2–8.

Figure 2 shows the space–time density wave evolution patterns of the new model when $\gamma = 0$, indicating that no preceding-lattice self-anticipative density integration information is considered. Specifically, figure 2(a) shows the density wave in the initial $t = 500$ time steps, and figure 2(b) reveals the density wave after $t = 500$ time steps. From Fig. 2, it can be seen that the initial disturbed stable traffic flow will evolve into traffic density wave and the oscillation of the density wave becomes more and more serious. Also, the final unstable traffic density wave takes on traffic density wave of high density region and that of low density region alternately. This density form can be described by the kink–antikink solution of the mKdV equation.

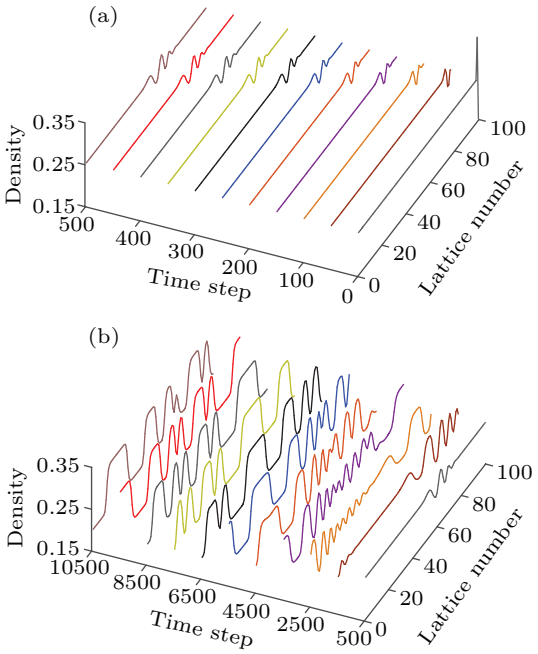


Fig. 2. Spatiotemporal evolution patterns of density wave when $\gamma = 0$.

Similarly, figures 3–5 describe the density evolution patterns of the new model obtained when $\gamma = 1$, and $m = 1$, 2, and 3 respectively. In Fig. 3, we find out that the initial stable traffic flow still becomes unstable under a disturbance, but the vibration level of the density wave is smaller than that in Fig. 2. It shows that the single-preceding-lattice self-anticipative density integration information can reduce the unstable level of traffic congestion. Furthermore, when two-preceding-lattice self-anticipative density integration effect is taken into account, we can see from Fig. 4 that the severity of traffic congestion has been lowered ulteriorly in comparison with Figs. 2 and 3. Finally, when three-preceding-lattice self-anticipative density integration effect is considered, it can be seen from Fig. 5 that the perturbation disappears in the traffic flow evolution process and the traffic flow recovers to the initial stable state. So, it is quite clear from Figs. 2–5 that the preceding-multiple-lattice self-anticipative density integration effect is very helpful in suppressing traffic congestion.

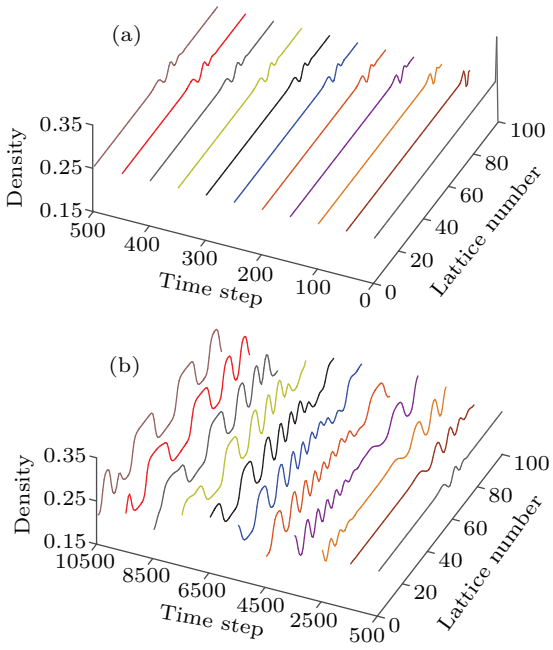


Fig. 3. Spatiotemporal evolution patterns of density wave when $\gamma = 1$ and $m = 1$.

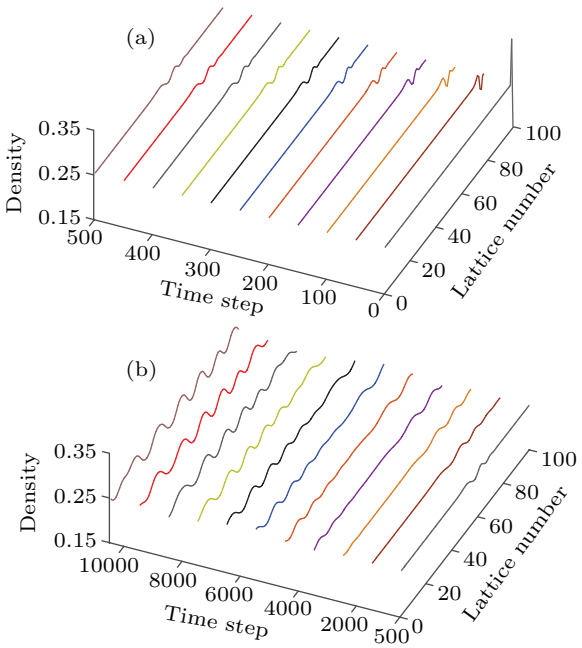


Fig. 4. Spatiotemporal evolution patterns of density wave when $\gamma = 1$ and $m = 2$.

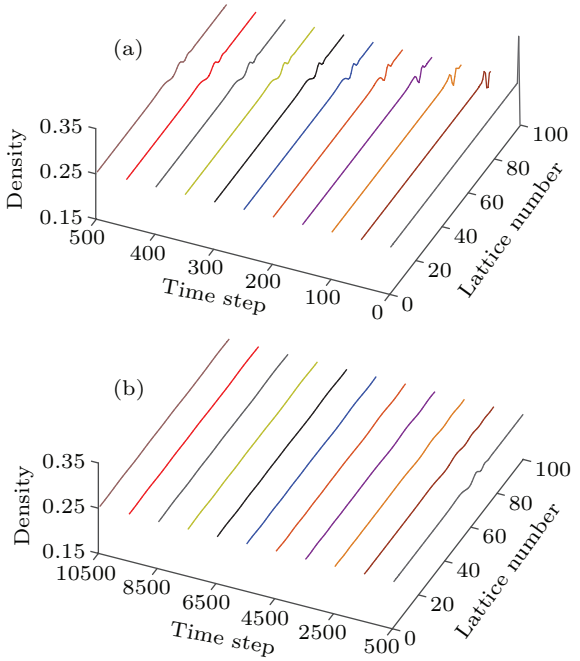


Fig. 5. Spatiotemporal evolution patterns of density wave when $\gamma = 1$ and $m = 3$.

Meanwhile, figure 6 describes the density evolution profiles of lattices $j = 90$, 80, and 70 at the first $t = 500$ time steps for different values of γ and m. The pattern in Fig. 6(a) corresponds to the case where no preceding-lattice self-anticipative density integration information is considered. The patterns in Figs. 6(b)–6(d) correspond to the situations where the preceding-lattice self-anticipative density integration information is considered, and the considered numbers of preceding lattices are $m = 1$, $m = 2$, and $m = 3$, respectively. In Fig. 6, in a short simulation time step, the outer side disturbance causes the initial stable traffic flow to evolve into a local fluctuation. The local fluctuation propagates backward from lattice $j = 90$ to $j = 70$. Also, the scale of the local fluctuation becomes smaller and smaller when the preceding-multiple-lattice self-anticipative density integration effect is taken into account by comparing the patterns in Figs. 6(a)–6(d).

Corresponding to Fig. 6, figure 7 provides the density evolution profiles of lattices $j = 90$, 80, and 70 in the time interval between $t = 9000$ and $t = 10000$ time steps under the same conditions. In Fig. 7, it is noted that the final traffic states, no matter whether it is stable or not, are quite similar to each other for lattices $j = 90$, 80, and 70 when the considered preceding-lattice number is fixed. This means that the traffic flow stability is a system-involved problem: it is independent of the selection of lattice number. In addition, by comparing the variation tendency of traffic states from the patterns in Fig. 7(a) to that in Fig. 7(d), it is shown that the unstable traffic flow has been alleviated gradually when more-preceding-lattice self-anticipative density integration information is considered, and the traffic congestion can completely be eliminated when three-preceding-lattice self-anticipative density integration information is taken into account.

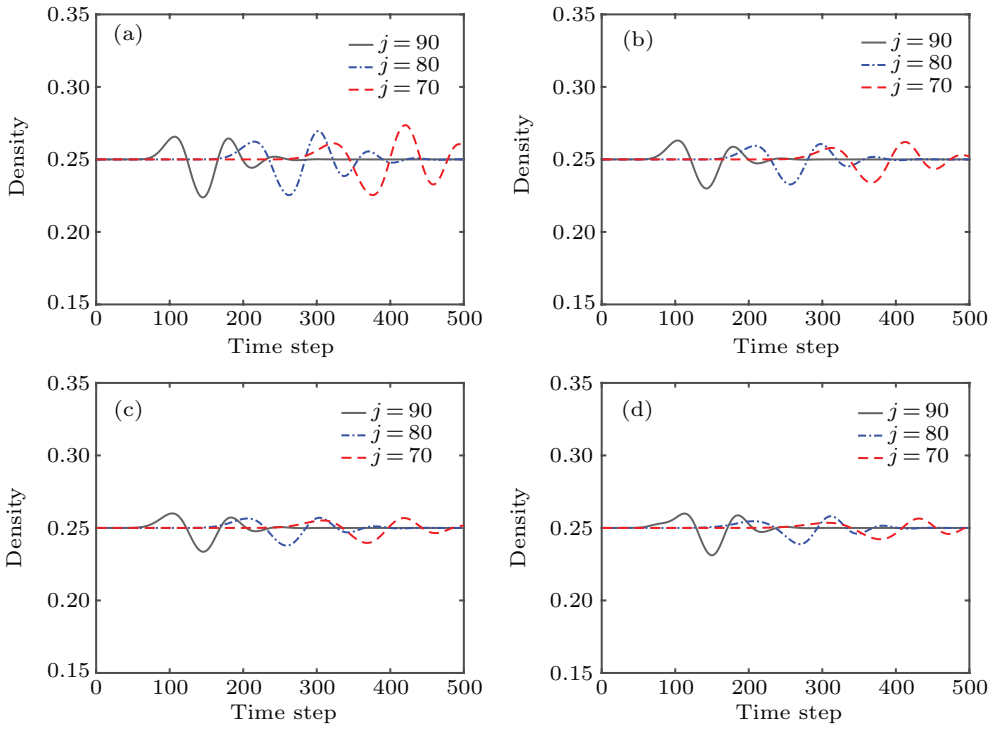


Fig. 6. Density evolution profiles of lattices $j = 90$, 80, and 70 at the first $t = 500$ time steps for different values of γ and m: (a) $\gamma = 0$, (b) $\gamma = 1$ and $m = 1$, (c) $\gamma = 1$ and $m = 2$, (d) $\gamma = 1$ and $m = 3$.

Figure 8 gives the density evolution profiles of lattices $j = 80$ from $t = 0$ and $t = 10000$ time steps corresponding to the cases where $\gamma = 0$ in Fig. 8(a), $\gamma = 1$ and $m = 1$ in Fig. 8(b), $\gamma = 1$ and $m = 2$ in Fig. 8(c), $\gamma = 1$ and $m = 3$ in Fig. 8(d). From

Fig. 8 we can see that the traffic evolution processes under a disturbance for different values of γ and m are quite different. The intensity of density wave fluctuation is the greatest when the preceding-lattice self-anticipative density integration is not taken into account. However, the unstable level of traffic density wave decreases gradually when the preceding-multiple-lattice self-anticipative density integration information is considered. When three-preceding-lattice self-anticipative density integration information is considered, the traffic density wave disappears. It further verifies the stabilization effect of multiple-lattice self-anticipative density integration on traffic flow.

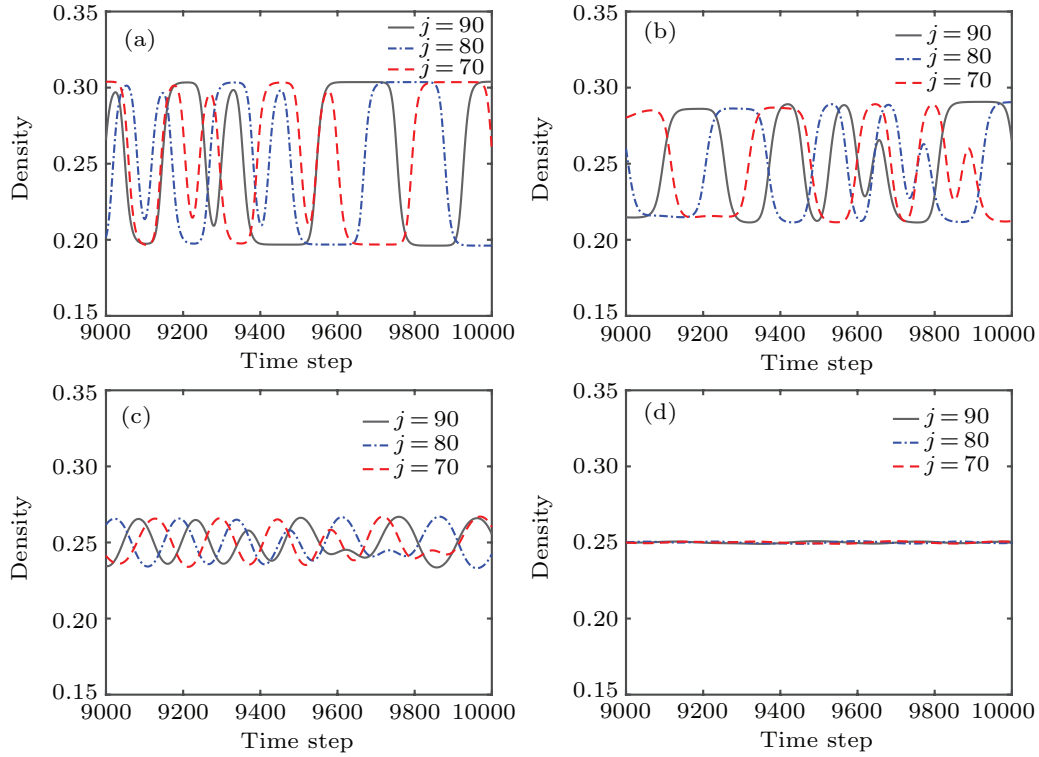


Fig. 7. Density evolution profiles of lattices $j = 90$, 80, and 70 from $t = 9000$ to $t = 10000$ time steps for different values of γ and m: (a) $\gamma = 0$, (b) $\gamma = 1$ and $m = 1$, (c) $\gamma = 1$ and $m = 2$, (d) $\gamma = 1$ and $m = 3$.

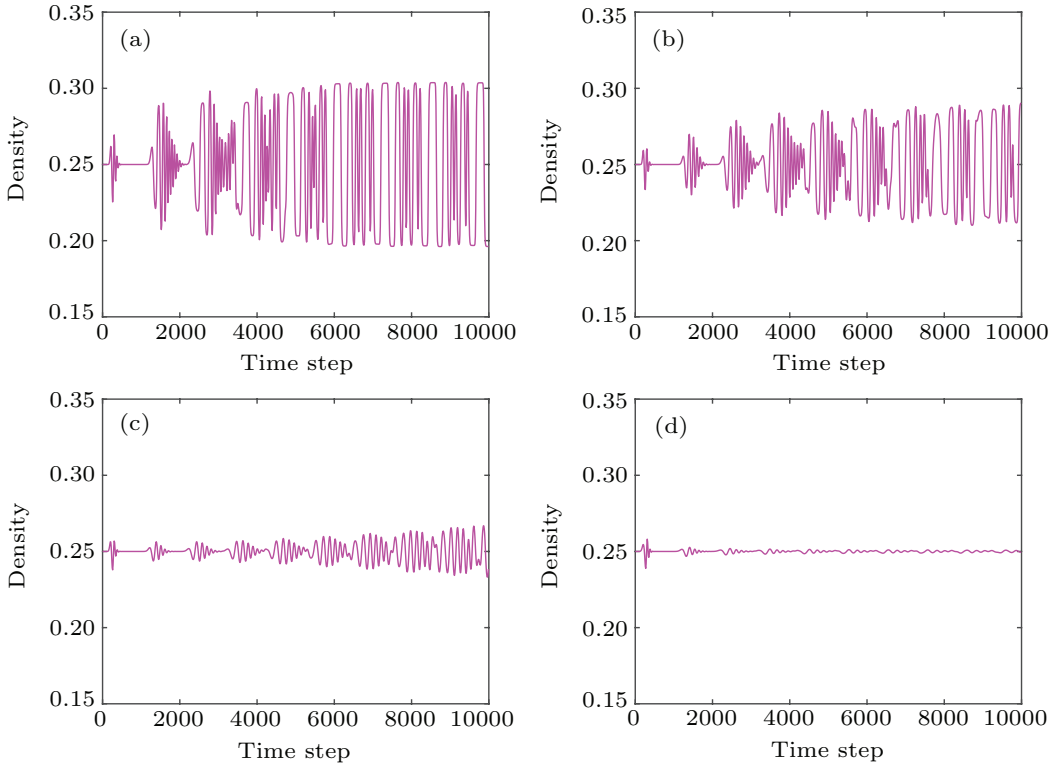


Fig. 8. Density evolution profiles of lattices $j = 80$ from $t = 0$ to $t = 10000$ time steps for different values of γ and m: (a) $\gamma = 0$, (b) $\gamma = 1$ and $m = 1$, (c) $\gamma = 1$ and $m = 2$, (d) $\gamma = 1$ and $m = 3$.

5. Conclusions

In this paper, a new traffic lattice hydrodynamic model is proposed to study the influence of multiple-lattice self-anticipative density integration on traffic flow in the V2V environment. Firstly, with the linear analysis method and the nonlinear analysis method, the new model's linear stability condition is derived and the propagation rule of the traffic density wave in the unstable region is revealed, respectively. It is shown that the unstable traffic density wave can be described by the solution of the mKdV equation. Then, through numerical simulation, the influence of multiple-lattice self-anticipative density integration on traffic stability is verified. The results show that multiple-lattice self-anticipative density integration effect can enhance the stability of traffic flow.

References

[1] Bando M, Hasebe K, Nakayama A, Shibata A and Sugiyama Y 1995 *Phys. Rev. E* **51** 1035
[2] Nagatani T 1998 *Physica A* **261** 599
[3] Dong C Y, Wang H, Wang W, Li Y and Hua X D 2018 *Acta Phys. Sin.* **67** 144501 (in Chinese)
[4] Peng G H 2020 *Chin. Phys. B* **29** 084501
[5] Chen Y and Zhang W 2020 *Acta Phys. Sin.* **69** 064501 (in Chinese)
[6] Jin Z Z, Cheng R J and Ge H X 2017 *Chin. Phys. B* **26** 110504 (in Chinese)
[7] Gupta A K, Sharma S and Redhu P 2014 *Commun. Theor. Phys.* **62** 393
[8] Wang T, Cheng R J and Ge H X 2019 *Physica A* **533** 121915
[9] Zhang Y C, Zhao M, Sun D H, Wang S H, Huang S and Chen D 2021 *Commun. Nonlinear Sci. Numer. Simul.* **94** 105541
[10] Sun F X, Chow A H, Lo S M and Ge H X 2018 *Physica A* **511** 389
[11] Ge H X and Cheng R J 2008 *Physica A* **387** 6952
[12] Tian J F, Yuan Z Z, Jia B, Li M H and Jiang G J 2012 *Physica A* **391** 4476
[13] Zhang Y, Wang S, Pan D B and Zhang G 2021 *Physica A* **561** 125269
[14] Kang Y R and Sun D H 2013 *Nonlinear Dynam.* **71** 531
[15] Wang T, Gao Z Y, Zhao X M, Tian J F and Zhang W Y 2012 *Chin. Phys. B* **21** 211
[16] Ge H X, Cui Y, Zhu K Q and Cheng R J 2015 *Commun. Nonlinear Sci. Numer. Simul.* **22** 903
[17] Li Y F, Zhang L, Zheng T X and Li Y G 2015 *Commun. Nonlinear Sci. Numer. Simul.* **29** 224
[18] Qin S D, Ge H X and Cheng R J 2018 *Phys. Lett. A* **382** 482
[19] Liu H, Sun D H and Liu W N 2016 *Physica A* **461** 795
[20] Pan D B, Zhang G, Jiang S, Zhang Y and Cui B Y 2021 *Physica A* **563** 125440
[21] Zhao H Z, Zhang G, Li W Y, Gu T L and Zhou D 2018 *Physica A* **503** 1204
[22] He Y C, Zhang G and Chen D 2019 *Int. J. Mod. Phys. B* **33** 1950071
[23] Wang Q Y and Ge H X 2019 *Physica A* **513** 438
[24] Qi X Y, Ge H X and Cheng R J 2019 *Physica A* **525** 714
[25] Liu C Q, He Y G and Peng G H 2019 *Physica A* **535** 122421
[26] Zhang G, Sun D H, Liu H and Chen D 2017 *Physica A* **486** 806